BNL-220581-2020-TECH

EIC-ESR-TN-010

Radial Shift Lattice Design using BMAD toolkit

H. Lovelace III

November 2020

Electron-Ion Collider Project

Brookhaven National Laboratory

U.S. Department of Energy

USDOE Office of Science (SC), Nuclear Physics (NP) (SC-26)

Notice: This technical note has been authored by employees of Brookhaven Science Associates, LLC under Contract No.DE-SC0012704 with the U.S. Department of Energy. The publisher by accepting the technical note for publication acknowledges that the United States Government retains a non-exclusive, paid-up, irrevocable, world-wide license to publish or reproduce the published form of this technical note, or allow others to do so, for United States Government purposes.

DISCLAIMER

This report was prepared as an account of work sponsored by an agency of the United States Government. Neither the United States Government nor any agency thereof, nor any of their employees, nor any of their contractors, subcontractors, or their employees, makes any warranty, express or implied, or assumes any legal liability or responsibility for the accuracy, completeness, or any third party's use or the results of such use of any information, apparatus, product, or process disclosed, or represents that its use would not infringe privately owned rights. Reference herein to any specific commercial product, process, or service by trade name, trademark, manufacturer, or otherwise, does not necessarily constitute or imply its endorsement, recommendation, or favoring by the United States Government or any agency thereof or its contractors or subcontractors. The views and opinions of authors expressed herein do not necessarily state or reflect those of the United States Government or any agency thereof.

Radial Shift Lattice Design using BMAD toolkit

H. Lovelace III, K. Dietrick, A. Drees, B. Gamage, C. Liu, Y. Luo, G. Marr, A. Marusic, F. Meot, R. Michnoff, S. Peggs, V. Ptitsyn, G. Robert-Demolaize, S. Verdu-Andres

Abstract

The electron-ion collider (EIC) conceptual design [1] requires that the hadron storage ring (HSR) be able to demonstrate radial shifts using a dual rigidity system. The dual rigidity system is a system in which the dipoles in the utility straight sections(USS) of the EIC lattice have a different rigidity than the arc dipoles thus affecting the beam orbit in the lattice arcs. This difference in rigidity allows the orbital offset in the arc magnets to reach approximately 18.7 mm offset, with a circumference lengthening of 73.2 mm.

1 Introduction

The electron ion collider design consists of the original relativistic heavy ion collider (RHIC) [2] arcs with redesigned USS. In the full on-energy injection scheme, with the energy range of 100 to 275 GeV/c for protons, the three outer (blue 11, yellow 1, and blue 3) and (yellow 7, blue 9, and blue 5) three inner arcs are used. For the 41 GeV configuration, the inner yellow 3 o'clock arc is used. The difference in circumference is approximately 90 cm for the 41 GeV case. The purpose of the radial shift is to synchronize the hadron storage ring to the electron storage ring by increasing or decreasing the particles path length in the arcs. For the radial shift, 24 correctors are also used to place the beam onto the dispersive orbit in the arc. In the following simulations, two sets of 24 correctors are used. One set is the arc dipole correctors(inner) and the other set is the USS correctors (outer). In the 6 o'clock interaction region (IR6) 4 arbitrary correctors were placed to flatten the orbit. The IR6 at the time of the study did not incorporate dipole correctors in the lattice. In all of the studies presented the BMAD toolkit [3] is used.

Table 1: Circumference lengthening and average radial shifts for hadrons at different energies. The circumference reduction required in the low energy 41 GeV configuration is achieved by passing hadrons through an additional inner arc bypass. ΔR is estimated using the formula $\Delta C = 2\pi\Delta R$

PROTONS

E_{tot} GeV	γ	$1-\beta$ 10^{-3}	C m	ΔC mm	$\langle\Delta R\rangle$ mm
41	43.70	0.2619	3832.863	-908.5	–
100	106.58	0.0440	3833.699	-73.2	-11.7
133	141.75	0.0249	3833.772	0.1	0.0
275	293.09	0.0058	3833.845	73.2	11.7

GOLD IONS

E_{tot} GeV/u	γ	$1-\beta$ 10^{-3}	C m	ΔC mm	$\langle\Delta R\rangle$ mm
40.7	43.70	0.2619	3832.863	-908.5	–
110	118.09	0.0359	3833.730	-41.9	-6.7

In BMAD, two method can be used to simulate the dual rigidity of the lattice. One method is using the patch at the beginning and end of each arc with the attribute controlling the total energy offset used. The patch element allows the energy, and thus the momentum, of the particle to be offset from the design reference energy of the lattice. The other method, which is explored in the note, is the attribute that allows a difference in the trajectory of a particle through a dipole magnet from the reference trajectory.

Rigidity is defined $(B\rho) = \frac{p}{q}$ where B is the magnetic dipole field, ρ is the radius of curvature, p is the momentum, and q is the charge of the particle. We can define the geometric strength of a dipole as $g = \frac{1}{\rho}$

Table 2: List of dipole correctors used in study.

Name (USS)	**s-coordinate (m)**	**Name (arc)**	**s-coordinate (m)**
IR8PRTH	125.000	YI6_TH11	172.396
IR7PRTH	140.000	YI6_TH13	201.983
YI7_TH9	497.865	YI7_TH13	438.679
YI7_TH7	527.290	YI7_TH11	468.266
BI8_TH7	749.671	BI8_TH11	808.695
BI8_TH9	779.096	BI8_TH13	838.282
BI9_TH9	1136.365	BI9_TH13	1074.979
BI9_TH7	1165.790	BI9_TH11	1104.566
BO10_TH6	1375.597	BO10_TH10	1434.689
BO10_TH8	1405.044	BO10_TH12	1464.346
BO11_TH8	1788.362	BO11_TH12	1731.261
BO11_TH6	1817.810	BO11_TH10	1760.918
YO12_TH6	2015.038	YO12_TH10	2071.930
YO12_TH8	2044.486	YO12_TH12	2101.587
YO1_TH8	2427.804	YO1_TH12	2368.502
YO1_TH6	2457.251	YO1_TH10	2398.159
BO2_TH6	2654.480	BO2_TH10	2713.572
BO2_TH8	2683.927	BO2_TH12	2743.230
BO3_TH8	3067.245	BO3_TH12	3010.144
BO3_TH6	3096.693	BO3_TH10	3039.801
BI4_TH7	3306.500	BI4_TH11	3365.523
BI4_TH9	3335.924	BI4_TH13	3395.110
IR9PFTH	3691.000	BI5_TH13	3631.807
IR8PFTH	3706.000	BI5_TH11	3661.394

and rewrite the magnetic field from the rigidity definition as B=$\frac{p}{q}$g. The magnetic field deviation, ΔB/B, can now be defined as ΔB/B = $\frac{p}{q}\times\Delta$g/g. In BMAD, we can write the dipole geometric field with its field difference as:

```
D: Sbend, L = 9.440656, G = 4.123021405059E-3, DG = 4.123021404998E-5
```

Another term will be introduced here, α_B geometric compaction. This term can be derived from the definition of momentum compaction α_c=ΔC/C$\div\Delta$p/p by substituting the ΔB/B for the momentum deviation.

$$\alpha_B = \Delta C/C \div \Delta B/B$$

The circumference lengthening is calculated using the time of flight of the particle, t_p, the time of flight of the reference particle, t_r and velocity of the particle, v_p.

$$\Delta C = (t_p - t_r) \times v_p$$

The beam pipe aperture in the arc dipoles is 3.46 cm. The radial shift limit for the arc dipole was selected as 20 mm due to the cryogenic heat load due to the resistive wall [4]. With the 20 mm radial shift, the the heat load will be increase by a factor of 13.4 over the average around the perimeter.

If achieving ΔB/B of 0.01 is too difficult, the phase advance per cell can be reduced. Dispersion in a FODO cell is defined as:

$$\eta_{\max} = L\Omega(\frac{1+\sin(\phi/2)/2}{4\sin^2(\phi/2)}$$

$$\eta_{\min} = L\Omega(\frac{1-\sin(\phi/2)/2}{4\sin^2(\phi/2)}$$

where L is the length of the FODO cell, Ω is the angle, ϕ is the phase advance.The maximum radial excursion is $R_{max} = \eta_{max} \times \Delta B/B$. If we define

$$Y = \eta_{max}/\eta_{min}$$

. We can then plot this ratio with respect to ϕ as shown in figure 2. An estimate of the gamma transition, γ_t, of the EIC hadron storage ring can be made from a single FODO cell. The momentum compaction of the FODO cell is:

$$\alpha_p = \int ds \eta_x/(\rho L)$$

with the assumption that there is no vertical dispersion. Gamma transition is then:

$$\gamma_t = 1/\sqrt{\alpha_t}$$

The increase of γ_t with increasing ϕ is shown in figure 2. In the EIC lattice, the reduction of ϕ is a strategy that is to be used only if radial shift difficulties are encountered.

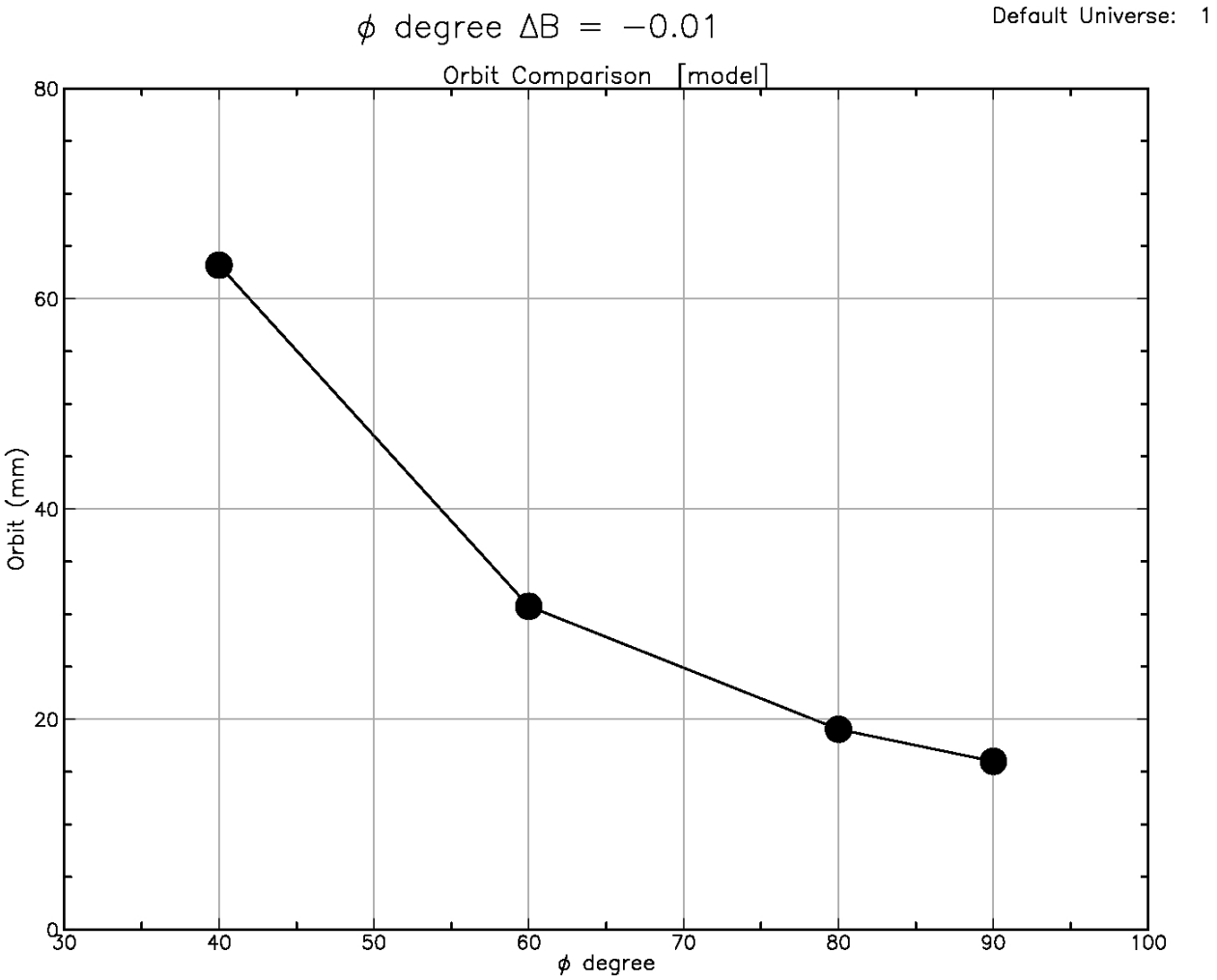


Figure 1: Maximum excursion in a FODO cell at -0.01 ΔB/B for increasing ϕ

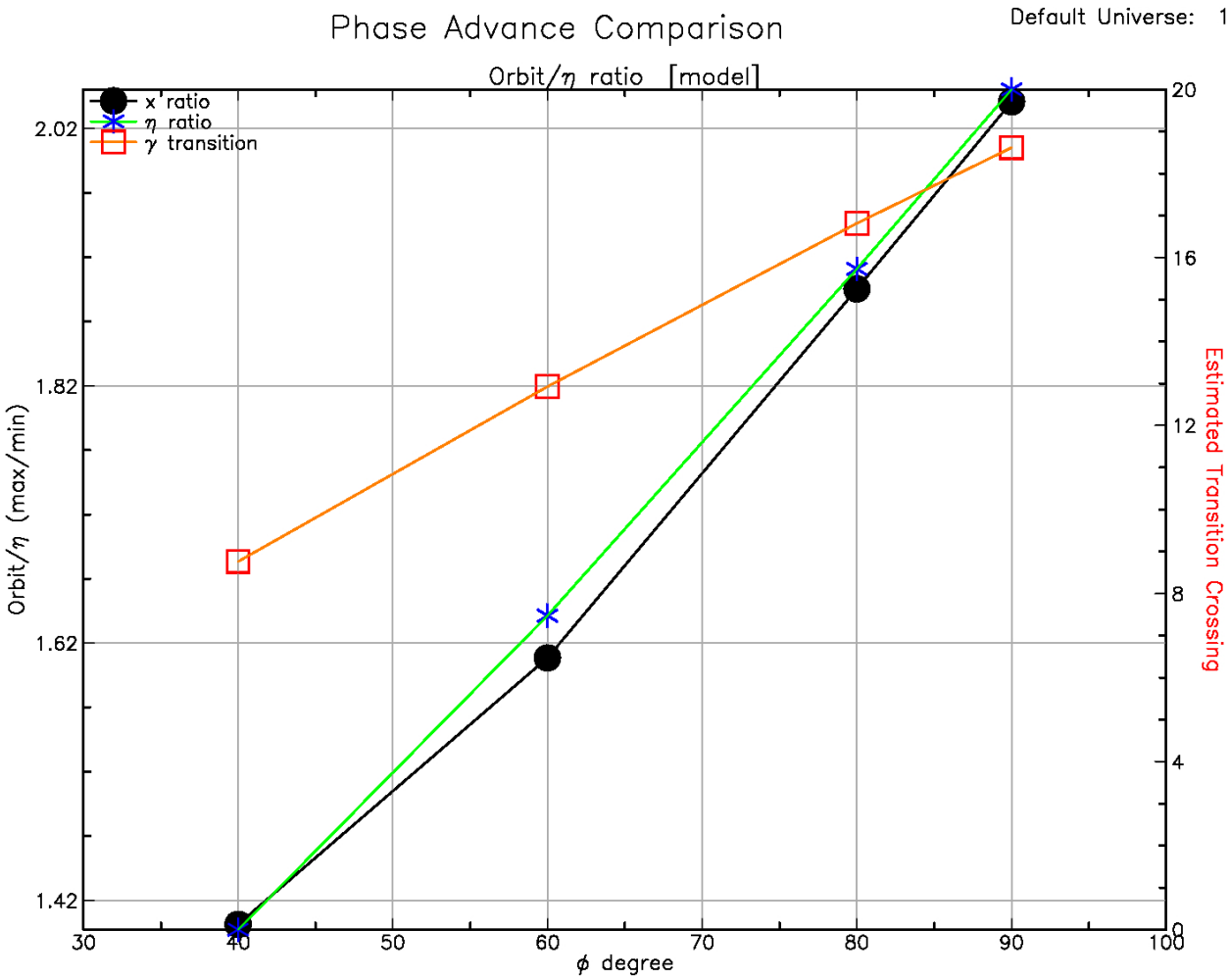


Figure 2: Change in dispersion and orbit max/min ratio at -0.01 ΔB/B for increasing ϕ. As the ϕ increases, γ_t increases.

2 Base Design Model

The base model for the study is v200512 version of the full energy injection lattice. The lattice path length circumference is 3833.860265 m, including the 5 mm bump in the proton forward side of the IR6. The horizontal and vertical tunes are 28.228 and 29.21, respectively. The chromaticity in both planes is 1 and the β^* at the IP is 80 cm horizontal and 7.2 cm vertically. The optics of the base lattice shown below in figure 3.

A metric in the lattice design is the β and dispersion waves in the arcs. Each inner and outer arc, when perfectly matched, mirrors the other inner or outer arcs. Unlike the RHIC, the USS do not have dipole crossover magnets (DX). The magnets are removed due to simplify the geometry and provide space for the electron storage ring crossover. The inner FODO cells have the ν_x of 0.229 and ν_y of 0.253. The outer FODO cells ν_x and ν_y of 0.230 and 0.254, respectively. $\nu_{x,y}$ is defined as:

$$\nu_{x,y} = \phi_{a,b}/(2\pi)$$

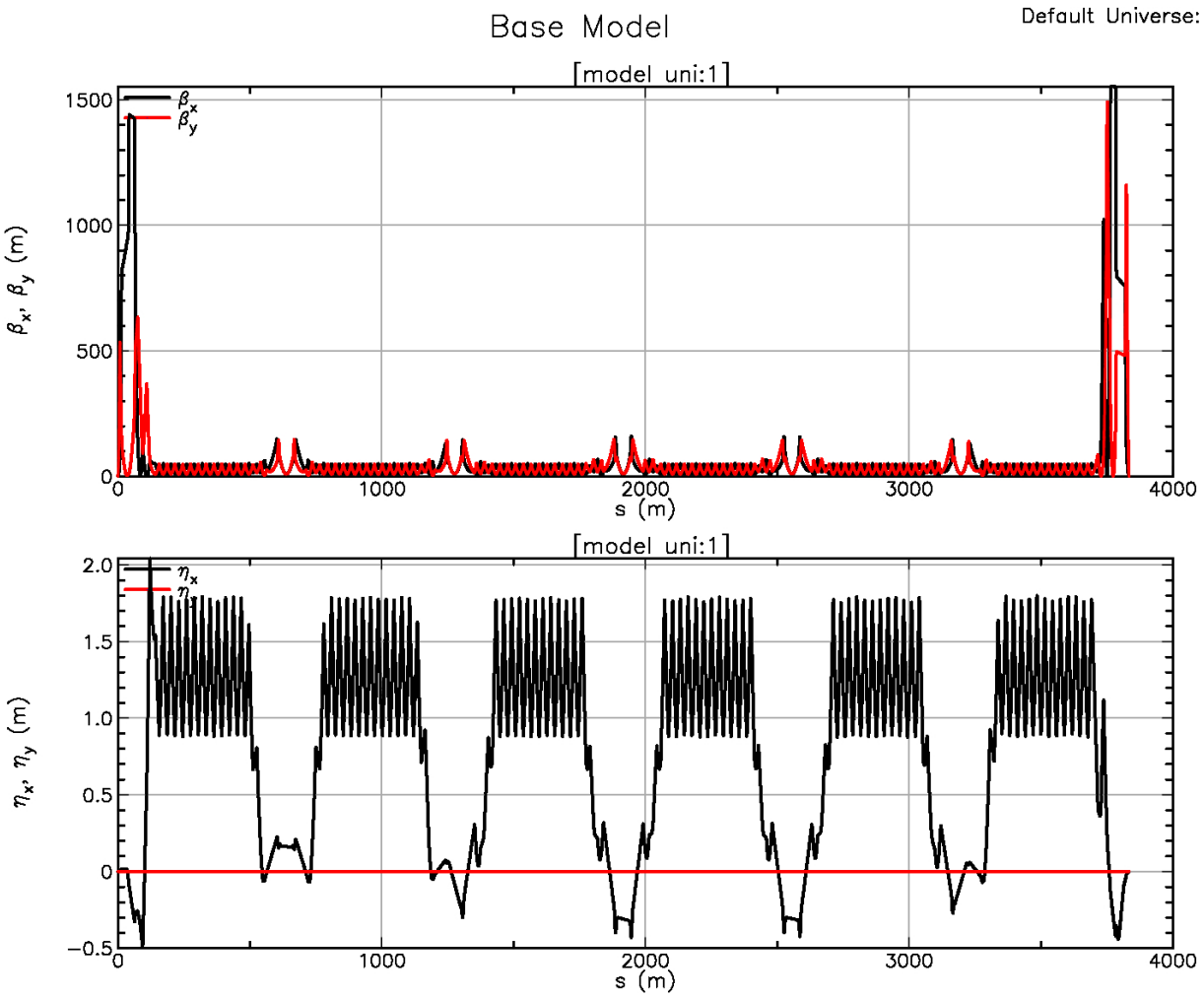


Figure 3: Base model with increasing s in clockwise direction

3 ΔB/B Lattices

Eight lattices, with ΔB/B of -0.01, -.005, 0.005, and 0.01 were created using a base model lattice. From the base model lattice, four lattices using arc (inner) dipole correctors and 4 lattices using USS outer correctors. The reasoning behind creating the multiple corrector configurations is that the objective is to satisfy the 73 mm circumference lengthening condition and with using only the arc dipole correctors, the 73 mm circumference lengthening objective may not be achievable without further lengthening schemes such as phase adjustments. Thus, the correctors in the USS may be used to increase the path length of the particle. Figures 8 through 12 show the β function of each individual arc using the USS correctors. The slight β waves may be corrected further by quadrupole and sextupole adjustments.

The radial shift causes a feed down effect [5] from the higher order magnetic elements in the arc. From Maxwell's Laws we have $\nabla \times \mathbf{H} = 0$ and $\nabla \times \mathbf{B} = 0$ for free space. The divergence of the magnetic induction is also zero. The magnetic inductance can be expressed as:

$$\mathbf{B} = -\nabla\phi_m$$

Laplace's equation for the scalar potential is $\nabla^2\phi_m = 0$. If cylindrical coordinates are chosen as the coordinate system the radial component of the magnetic inductance can be written as:

$$B_r(r,\theta) = -(\frac{\partial\phi_m}{\partial r}) = \sum_{n=1}^{\infty} C(n)(\frac{r}{R_{ref}})^{n-1}\sin(n(\theta-\alpha_n))$$

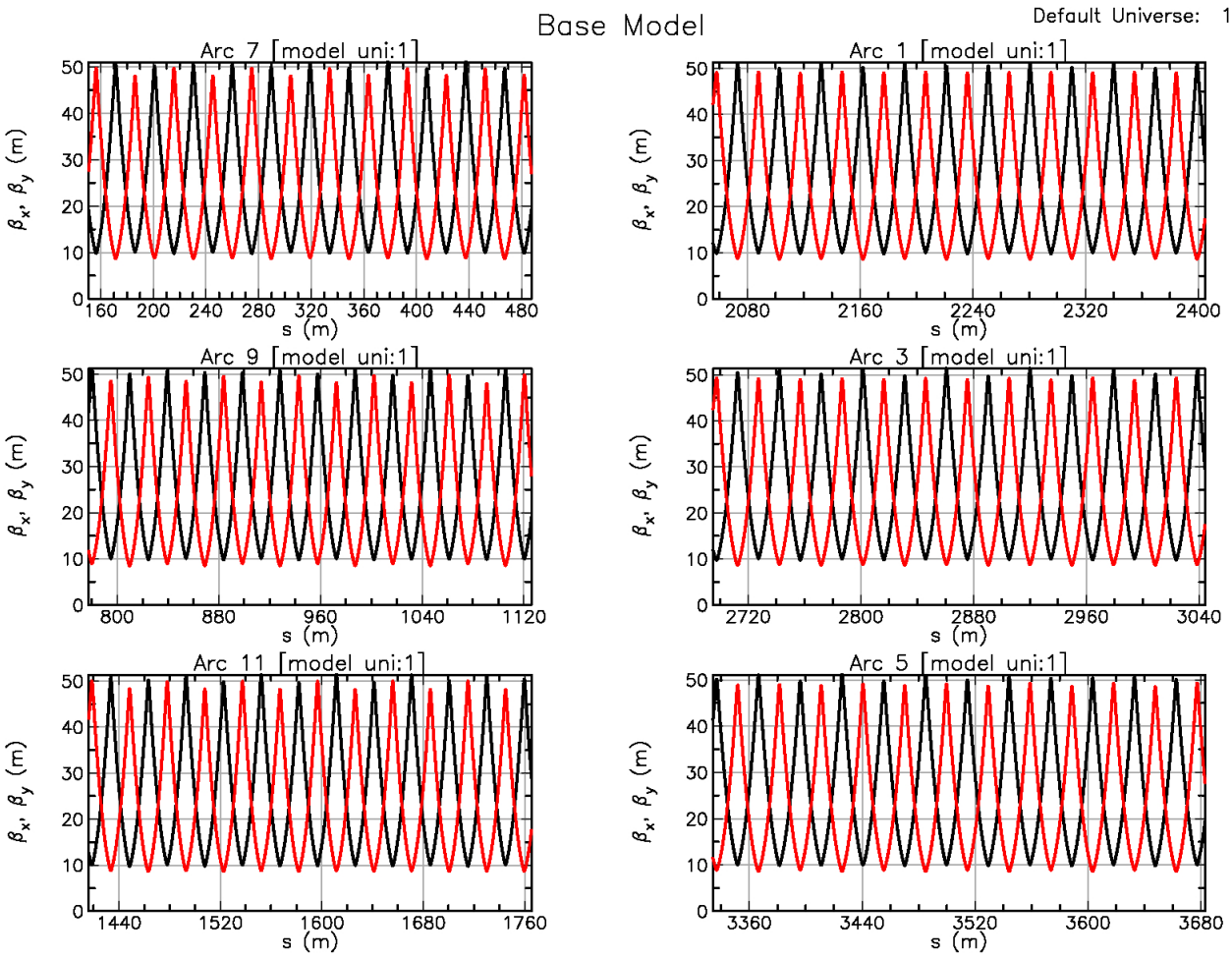


Figure 4: Base model arc β functions

$$B_\theta(r,\theta) = -\frac{1}{r}(\frac{\partial \phi_m}{\partial \theta}) = \sum_{n=1}^{\infty} C(n)(\frac{r}{R_{ref}})^{n-1}\cos(n(\theta-\alpha_n))$$

where R_ref is the reference radius, C(n) is the amplitude and α_n the phase angle. Both are constants. θ is the position of the magnetic poles. $B_{r,\theta}(r,\theta)$ can be written in as the complex field $\mathbf{B(z)}$:

$$\mathbf{B(z)} = B_y(x,y) + iB_x(x,y) = \sum_{n=1}^{\infty} C(n)e^{-in\alpha_n}(\frac{z}{R_{ref}})^{n-1}$$

$\mathbf{B(z)}$ can be expanded into normal and skew components:

$$\mathbf{B(z)} = B_y + iB_x = \sum_{n=0}^{\infty}(B_n + iA_n)(\frac{z}{R_{ref}})^n$$

If a translation in done from one frame to the other, the translated magnetic induction, $\mathbf{B(z')}$, can be written as:

$$\mathbf{B(z')} = \sum_{n=0}^{\infty}[\sum_{k=n}^{\infty}(B_k + iA_k)\frac{k!}{n!(k-n)!}(\frac{z_0}{R_{ref}})^{k-n}](\frac{z'}{R_{ref}})^n$$

$$= \sum_{n=0}^{\infty}(B'_n + iA'_n)(\frac{z'}{R_{ref}})^n$$

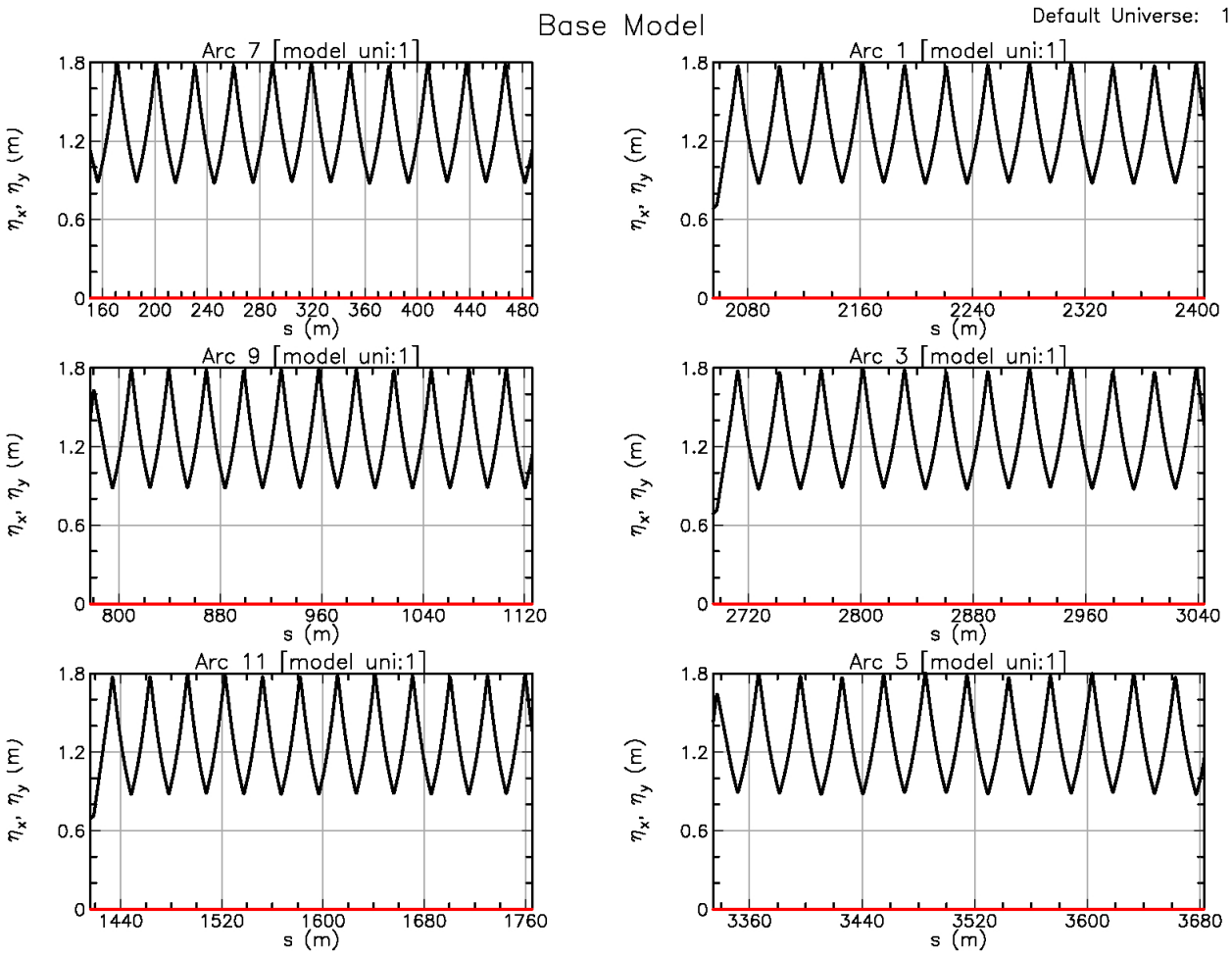


Figure 5: Base model arc η functions

In the translated frame the expansion coefficients can be written as:

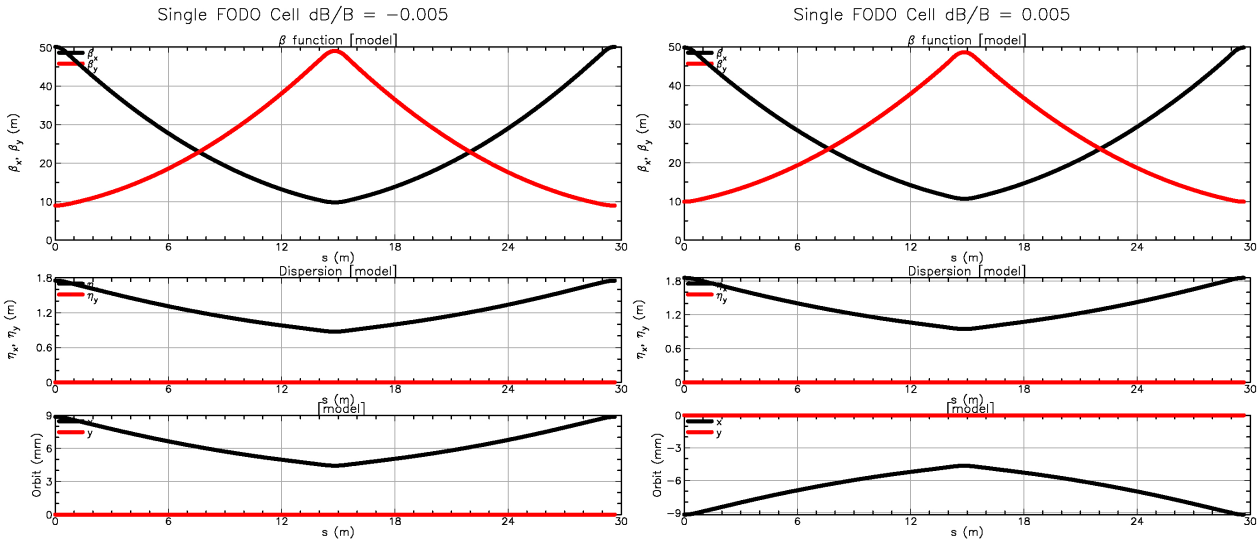
$$(B'_n + iA'_n) = \sum_{n=0}^{\infty}[(B_k + iA_k)[\frac{k!}{n!(k-n)!}](\frac{x_0 + iy_0}{R_{ref}})^{k-n}]$$

with the amplitude and phase angle given by:

$$C'(n)e^{-in\alpha'_n} = \sum_{k=n}^{\infty}[C(k)e^{-ik\alpha'_k}[\frac{(k-1)!}{(n-1)!(k-n)!}](\frac{x_0 + iy_0}{R_{ref}})^{k-n}]$$

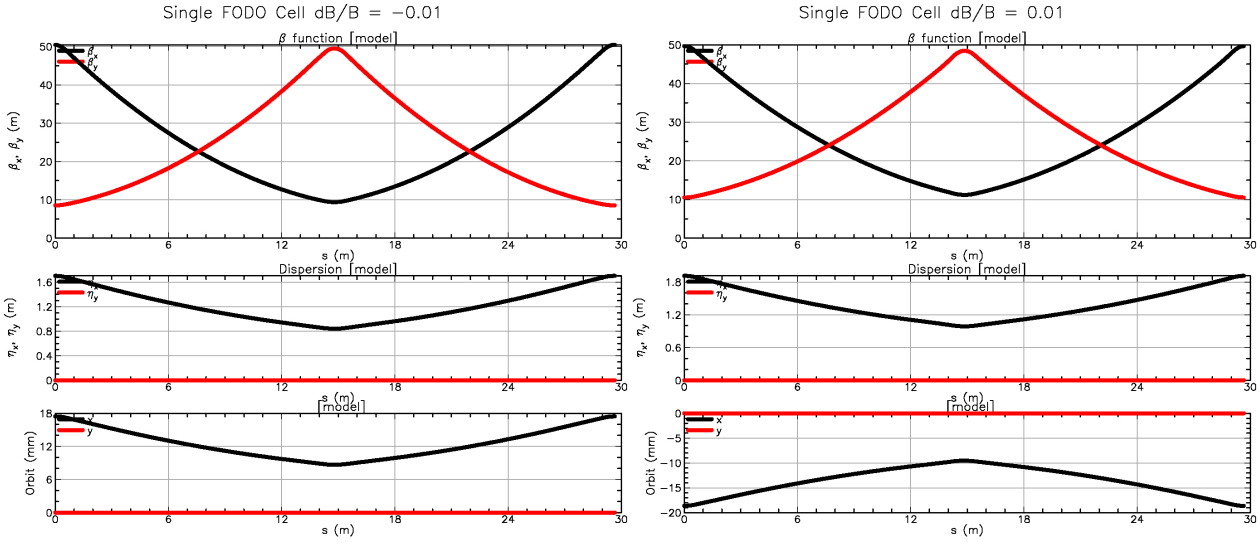
To create the radially shifted lattices, first the closed periodic solution for the lattice is found for a given ΔB/B. Figures 6 and 7 show the β functions, dispersion, and orbit excursion for each of the ΔB/B configurations. Once the closed solution is found, the USS is then rematched to the arc cell closed solution using the USS quadrupoles. In each USS there are 18 quadrupoles and with 2 sets of triplets located between the D0 dipole magnets. The β^* in USS are constrained to be 10 m in both planes.

In each lattice ΔB/B configuration, the USS and IR6 (for USS correctors) and the outer most FODO cells of arcs (for arc correctors), are optically matched to the closed solution of the FODO cells. In BMAD, a useful feature that was used in these simulations is the ability to slice a lattice into segments. The initialization file of the Tool for Accelerator Optics (TAO) must include the following syntax to "slice" the lattice and only observe the individual FODO cell.



(a) -0.005 ΔB/B (b) 0.005 ΔB/B

Figure 6: Example of Single FODO cell at ±0.005 dB/B



(a) -0.01 ΔB/B (b) 0.01 ΔB/B

Figure 7: Example of Single FODO cell at ±0.01 ΔB/B

```
&tao_design_lattice
  n_universes = 3
  design_lattice(1) = "0db.bmad" !lattice name
  design_lattice(2) = "0db.bmad" !lattice name
  design_lattice(2)%slice_lattice = "YI7_QF21:241" !inner arc FODO cell
  design_lattice(3) = "0db.bmad"
  design_lattice(3)%slice_lattice = "YO1_QF20:2082" !outer arc FODO cell
/
```

The lattice filename nomenclature is as follows:

Nominal Lattice	0db.bmad
USS -0.01 ΔB/B	n1db.bmad
USS -0.005 ΔB/B	np5db.bmad
USS 0.005 ΔB/B	p5db.bmad
USS 0.01 ΔB/B	1db.bmad
Arc -0.01 ΔB/B	inner_corr_n1db.bmad
Arc -0.005 ΔB/B	inner_corr_np5db.bmad
Arc 0.005 ΔB/B	inner_corr_p5db.bmad
Arc 0.01 ΔB/B	inner_corr_1db.bmad

Each EIC arc, has a total of 11 of these FODO cells. The particle orbit will follow the dispersion.Using Hill's equation, the relationship between the geometric orbit and dispersion can be derived as

$$x_{co} = -\eta \times \Delta B/B$$

$$x'_{co} = -\eta' \times \Delta B/B$$

The maximum orbit excursion occurs in the lattices where the ΔB/B is the greatest. The maximum excursions, circumference lengthening, and α_B for a given ΔB/B are shown in table 3. As shown in the table, the using the USS correctors gives a approximately 20% increase in the circumference lengthening. Results are comparable to the results from a similar study of circumference lengthening using Zgoubi [6]. The optics for each ΔB/B case are shown in figures 8 through 12. A comparison in the orbits for the USS corrector and arc corrector configuration are shown in figures 14 through 19.

Table 3: Comparison of ΔB/B, ΔC, and α_B to the maximum excursion in arc(lengths are in mm, α_B is multiplied by 10^{-3})

ΔB/B	**-0.01**	**-0.005**	**0.005**	**0.01**
Inner (arc) correctors mm,mm	18.5, 58.95, -1.54	9.4, 28.84, -1.50	-9.1, -28.25, -1.47	-18.9, -55.33, -1.44
Outer (USS) correctors mm,mm	18.7, 73.20, -1.91	9.6, 35.86, -1.87	-9.3, -34.17, -1.78	-18.9, -66.96, -1.75

4 Conclusion

The use of dual rigidity for a given EIC lattice is a viable method of circumference lengthening. The circumference is lengthened by 73.2 mm for -0.01 ΔB/B with the use of the USS correctors and 58.95 mm with the use of the arc correctors. For 0.01 ΔB/B, the circumference is lengthened by -66.96 mm (USS) and -55.33 mm (ARC).

5 Acknowledgements

Special thanks to J.S. Berg for useful conversations about BMAD optimization and IR 6 development. Thank you to David Sagan who was always available for BMAD discussions and changes to source code that were made to accommodate this particular radial shift interest.

References

[1] EIC collaboration, *Electron-Ion Collider at Brookhaven National Laboratory Conceptual Design Report*. Collider-Acclerator Department, Upton,NY, 17 ed., October 2020. pages 183-189.

[2] Accelerator Division, *RHIC:relativistic hadron ion collider configuration manual*. Collider-Accelerator Department, Upton,NY, 4 ed., November 2006.

[3] D. Sagan, "Bmad: A relativistic charged particle simulation library," *Nucl. Instrum. Meth.*, vol. A558, no. 1, pp. 356–359, 2006. Proceedings of the 8th International Computational Accelerator Physics Conference.

[4] S. Verdú-Andrés, "Resistive wall heating in the copper-coated beam pipe of the BNL Electron-Ion Collider," Tech. Rep. 219910, Brookhaven National Laboratory, Upton,NY, September 2020. EIC-ADD-TN-008.

[5] A. K. Jain, "Basic theory of magnets," in *Proc. CERN Accelerator School on Measurement and Alignment of Accelerator and Detector Magnets*, 1997.

[6] F. Méot, R. Robert-Demolaize, "Radial-Offset Optics in EIC Hadron Lattices. Trajectory Lengthening," Tech. Rep. 6, Brookhaven National Laboratory, Upton,NY, August 2020. EIC-ADD-TN-006.

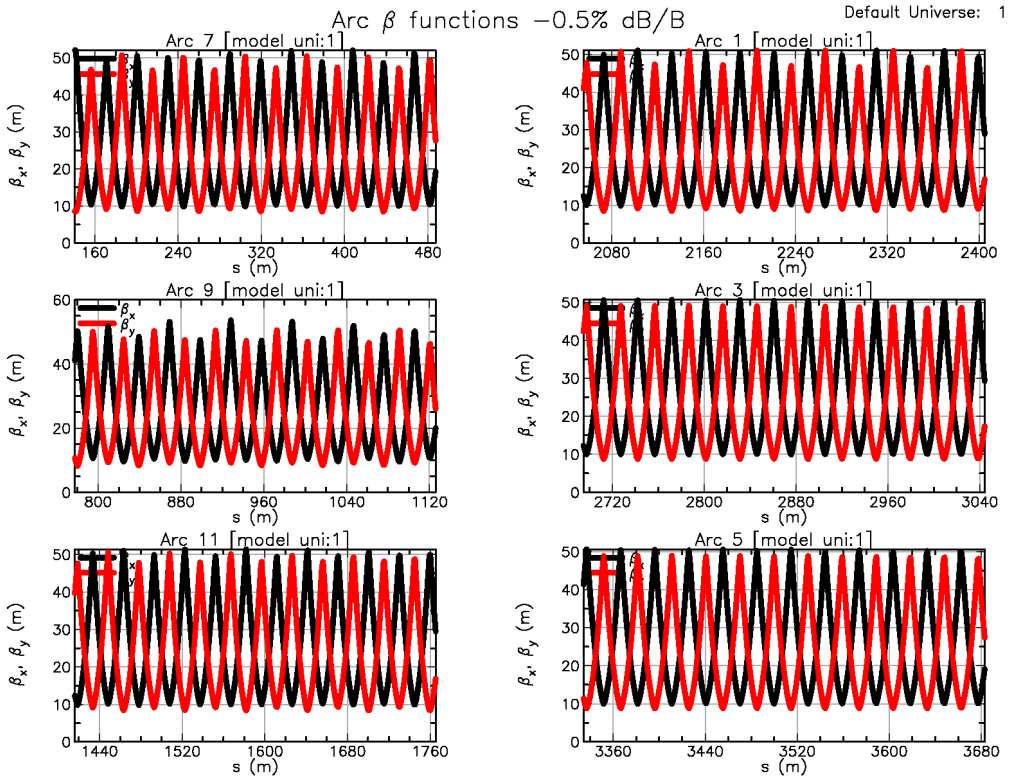


Figure 8: -0.005 ΔB/B

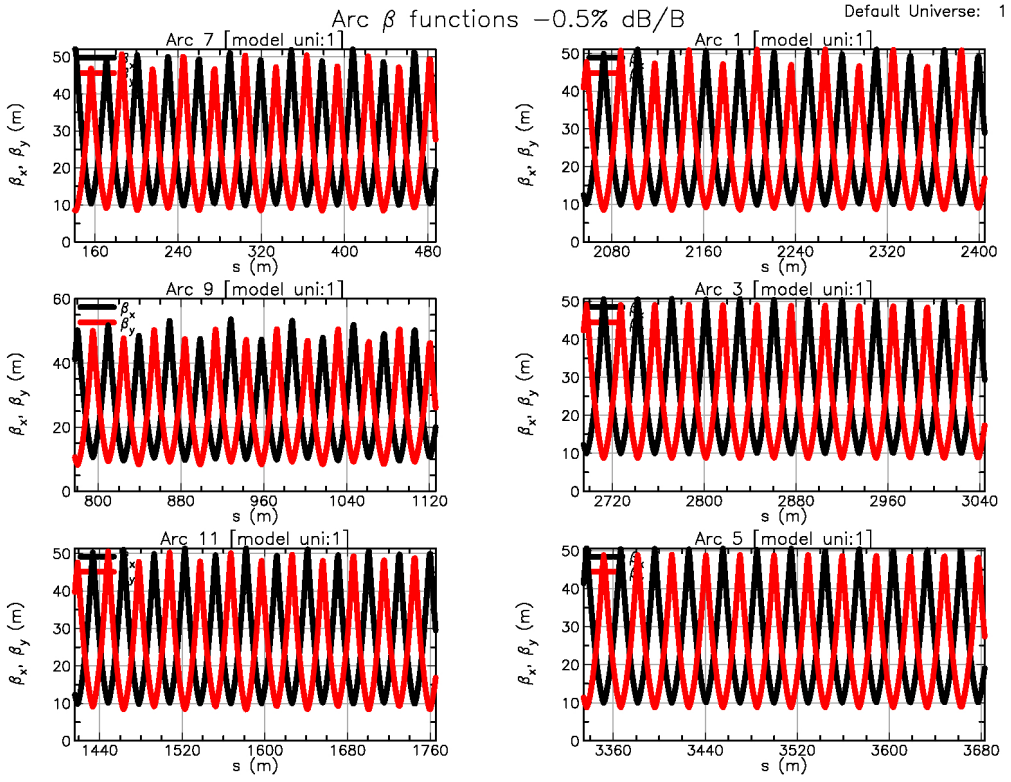


Figure 9: 0.005 ΔB/B

Figure 10: Arc β functions with USS corrector configuration $\pm 0.005 \Delta B/B$

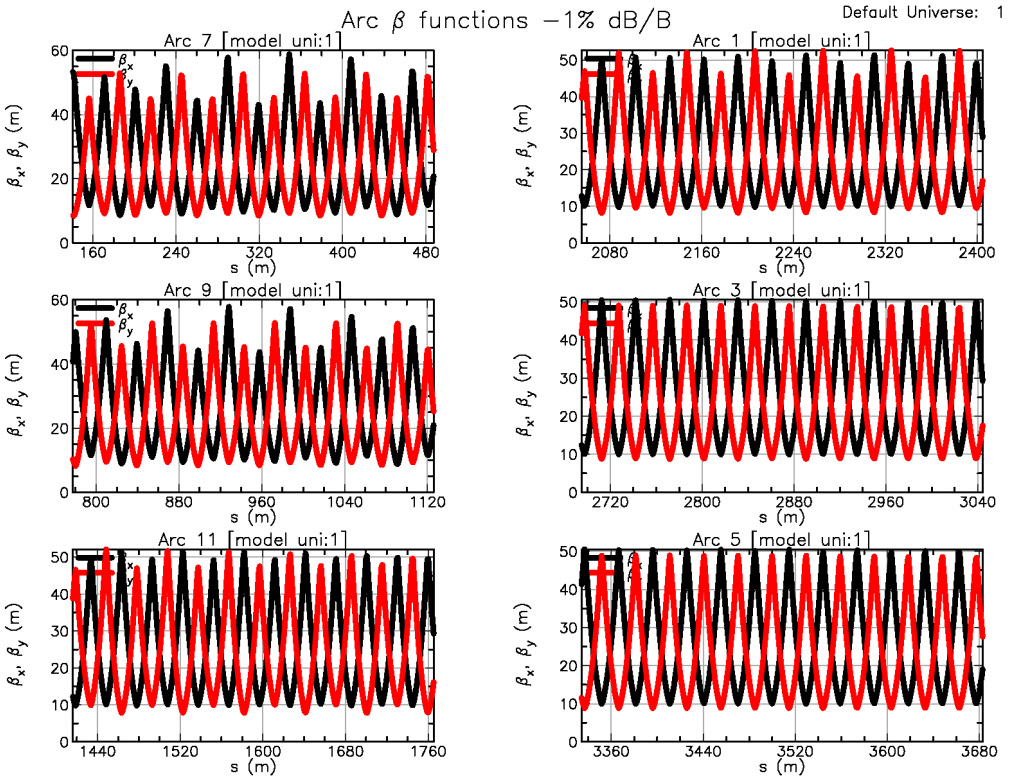


Figure 11: -0.01 ΔB/B

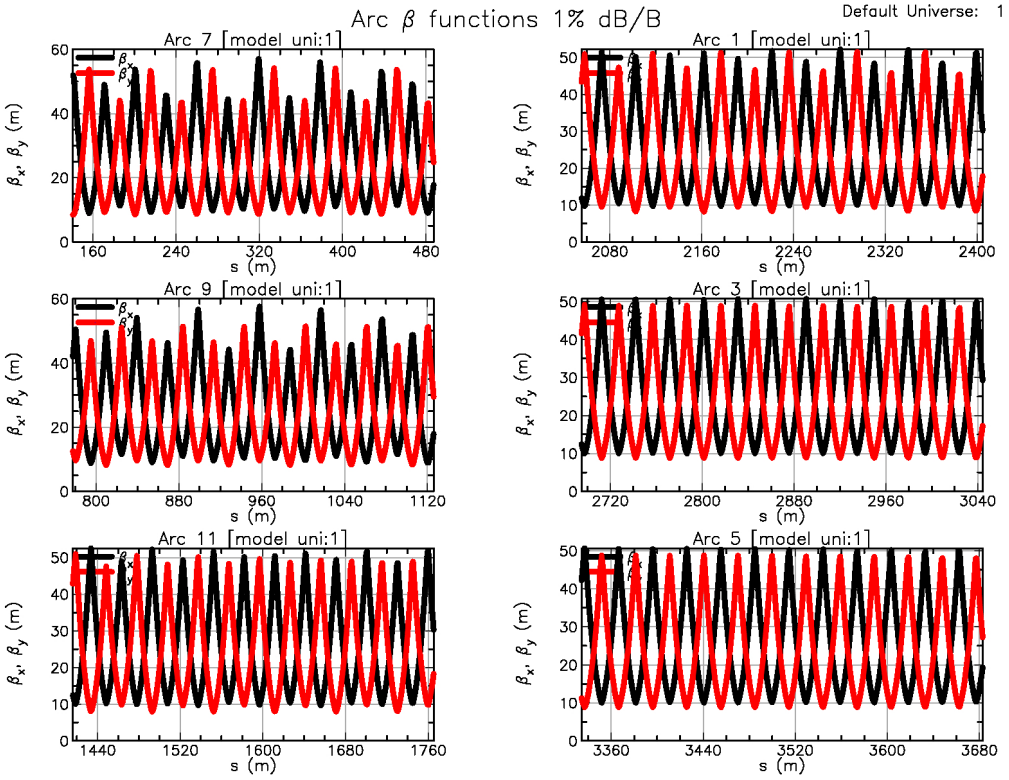


Figure 12: 0.01 ΔB/B

Figure 13: Arc β functions with USS corrector configuration $\pm$0.01 ΔB/B

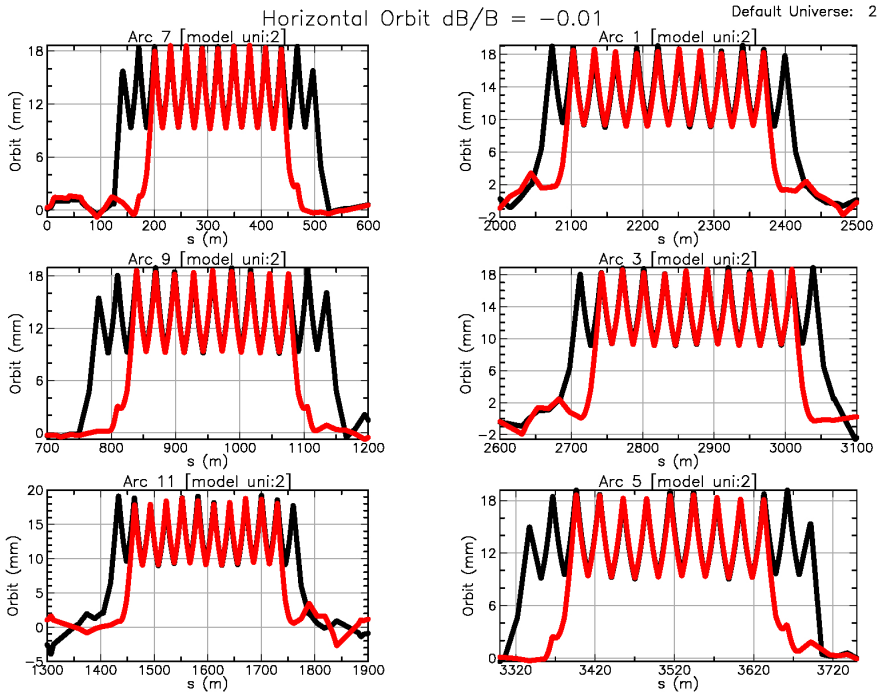


Figure 14: -0.01 ΔB/B

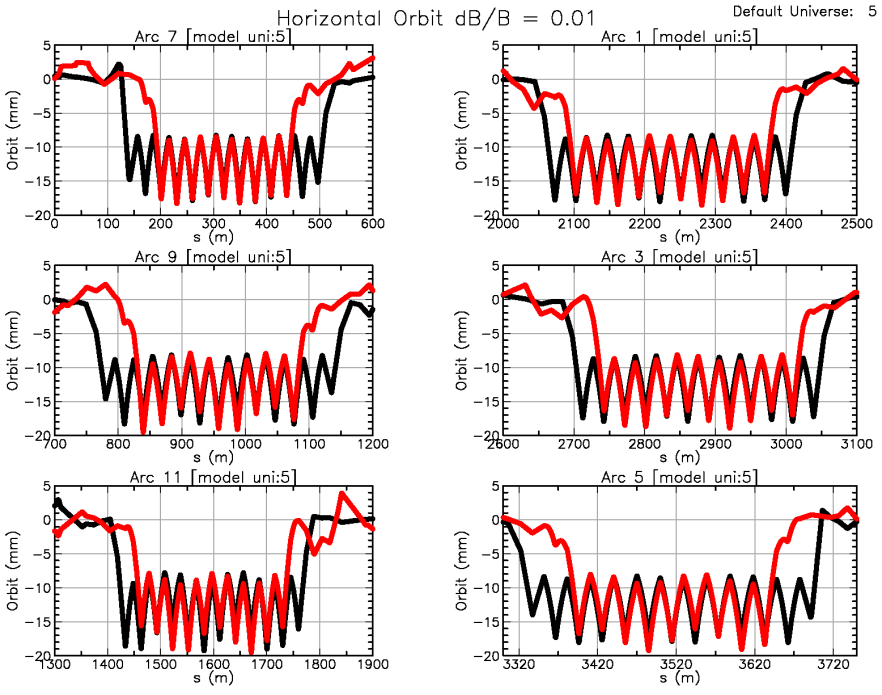


Figure 15: 0.01 ΔB/B

Figure 16: Arc orbit comparison black USS correctors rad arc correctors ±0.01 ΔB/B

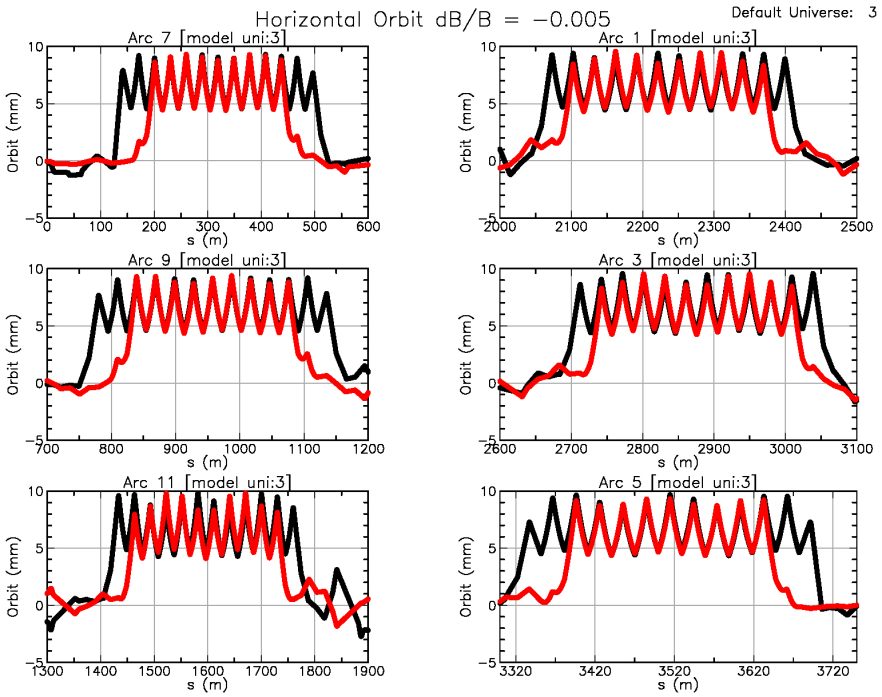


Figure 17: -0.05 ΔB/B

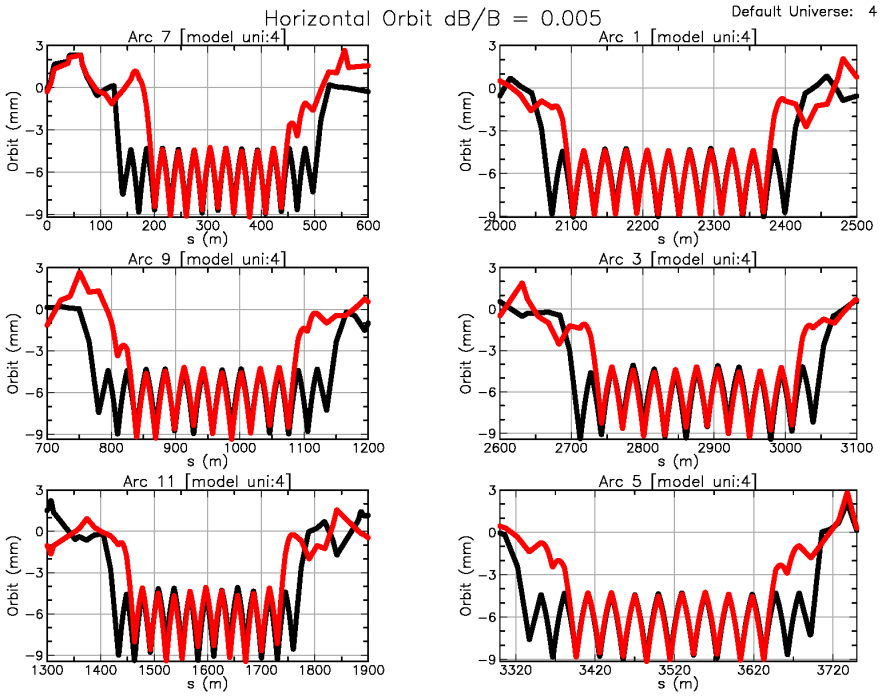


Figure 18: 0.05 ΔB/B

Figure 19: Arc orbit comparison black USS correctors rad arc correctors ±0.05 ΔB/B